ELSEVIER

Journal of Molecular Liquids 70 (1996) 185–198

journal of MOLECULAR LIQUIDS

Density dependence of the structural properties and translational diffusion of Carbonyl Sulphide diluted in monoatomic solvents. A Molecular Dynamics investigation.

D. Dellis and J. Samios[1]
Department of Chemistry, Laboratory of Physical Chemistry, University of Athens, Panepistimiopolis 157-71 Greece

Abstract

We report a study of the intermolecular structure and translational diffusion of Carbonyl Sulphide (OCS) dissolved in Ne and Kr, using Molecular Dynamics (MD) simulation. The mixtures have been investigated at different thermodynamic points corresponding to the pressures between 5 and 300 bar and at temperature of 293 K. The computations were carried out with effective site-site Lennard-Jones (LJ) potential model. We found that the proposed model predicts a non-linear T-shaped dimer structure of Ne-OCS and Kr-OCS in accordance with experiment. The study of the local structure of the solute-solvents was based upon the calculated relevant pair distribution functions. The self-diffusion coefficients of both components in the mixtures were calculated and compared. The results show a non-linear dependence in the density range under study. In the case of Kr as solvent and at the whole density range under study, the diffusion coefficient of Kr appears to be larger than that of OCS. This unusual result on the solute-solvent diffusivities ($m_{OCS} < m_{Kr}$, $D_{OCS} < D_{Kr}$) has been further discussed in terms of the microscopic dynamics of the species.

1. INTRODUCTION

In two recent publications [1, 2], hereafter referred as I and II, the molecular dynamics simulation (MD) technique was applied to study the density dependent properties of carbonyl sulphide (OCS) diluted in argon (Ar). Information regarding the microscopic intermolecular structure and the dynamics of the molecular motion of OCS perturbed by Ar atoms was obtained and analyzed. Furthermore, we found that the calculated reorientational first order Legendre autocorrelation functions (ACFs) corresponding to the ν_1 and ν_3 fundamental bands of OCS in Ar [2] are in quite good agreement with the experimental ACFs obtained from infrared (IR) spectra in previous studies [3–5].

In the present work, we continue our systematic investigation on the properties of OCS diluted in dense rare gases and liquid solvents. Here, we shall describe the MD simulation study of the dilute mixtures of OCS in Krypton and Neon which, as far as we know, is the first study on these molecular systems within the framework of this method. Attention will be paid to the behavior of the translational diffusion coefficients of the linear molecules in the mixtures as a function of density.

[1]Corresponding Author

PII S0167-7322(96)00967-1

On the experimental side, both mixtures have been investigated by conventional infrared spectroscopy [4, 6]. In these studies the band profiles of the fundamental vibrational frequencies ν_1, ν_2 and ν_3 of the OCS molecule perturbed by these atoms have been studied in a wide density range and in terms of the determined reorientational ACFs and of the two normalized spectral moments M(2) and M(4). On the basis of these results the authors pointed out that the mean squared torque on OCS molecules varies as a function of density. Also, they found that the rotational motion becomes significantly restricted by increasing the density.

On the other hand, it is well known that rotational-vibrational spectroscopy on weakly bound van der Waals complexes has provided helpful information on their molecular properties and on the most stable dimer structure [7]. Experimental work published in this area includes pulsed beam Fourier transform microwave [8] and molecular beam infrared absorption [9] techniques.

For each of the rare gas-OCS weak complexes, the estimated dimer structure was found to be T-shaped and the characteristic structural parameters have been reported.

The first part of this treatment deals with the interactions involving pairs of unlike molecules in the mixtures. In fact, we are interested to construct effective potentials which will enable us to predict the experimentally accessible thermodynamic, structural and dynamical properties of the systems.

In the following sections the MD simulations will be presented and the obtained results will be discussed and compared with corresponding experimental data. Finally, the main conclusions pointed out from these studies will be summarized.

2. COMPUTATIONAL ASPECTS AND POTENTIAL MODELS

The MD simulations were carried out in the microcanonical ensemble with systems of 10 linear triatomic OCS molecules dissolved in 490 Kr or Ne atoms in a cubic box with the usual periodic boundary conditions.

The fundamental technical details applied in the present simulations have been used and described at length in our previous papers I and II. We must note, however, that after equilibration each MD run was extended up to 640 ps with integration time step $3.2 \cdot 10^{-15}$ s. The total energy drift was lower that $10^{-4} KJ/mol$ for all MD runs.

The thermodynamic states considered for the simulated mixtures were chosen to make possible comparisons with results obtained in previous experimental studies. In all simulations, the initial temperature was 293 K and the mixtures have been simulated at 13 different densities corresponding to the pressures between 5 and 300 bar. Moreover, in order to compare the predicted results at equal molar volumes, we have investigated the systems at four additional state points. The investigated state points (P,V,T) and the calculated macroscopical properties are summarized in table 1.

Table 1
MD results for the diluted mixtures OCS-Kr, OCS-Ne (mole fraction OCS : 0.02). Depicted are the molar volumes V_m [4] and the equilibrium properties : Temperature T,potential energy U_p, Pressure P, mean squared forces $\langle F^2 \rangle$, and torques $\langle N^2 \rangle$ and the calculated translational diffusion coefficients of the molecular dynamics runs 1-17. The numbers in parentheses are the experimental pressure of pure Kr and Ne at temperature 298 K [19, 20, 22, 23].

MD	V_m	T	$-U_p$	P	$\langle F^2 \rangle_{R.g.}$	$\langle F^2 \rangle_{OCS}$	$\langle N^2 \rangle_{OCS}$	D_{OCS}	$D_{R.g.}$
Run	$[cm^3]$	$[K]$	$[\frac{KJ}{mol}]$	$[bar]$	$[10^{-20}N^2]$		$[10^{-40}J^2]$	$10^{-4}\frac{cm^2}{sec}$	
					OCS-Kr				
1	81.5	295.6	3.35	215	2.21	3.80	4.73	2.04	2.52
2	104.3	292.8	2.69	164	1.68	2.98	3.81	2.79	3.33
3	124.6	293.5	2.30	140	1.40	2.45	3.09	3.65	3.95
4	166.1	293.6	1.74	111(115)	1.01	1.83	2.30	4.26	5.10
5	224.2	294.1	1.30	89	0.75	1.28	1.57	4.66	6.49
6	560.5	292.1	0.53	40	0.29	0.54	0.69	11.07	12.39
7	4484.3	292.6	0.07	5.3	0.04	0.05	0.06	34.30	43.15
8	280.0	292.5	1.03	72(74)	0.58	1.03	1.35	7.85	9.40
9	41.7	292.4	6.39	1267	6.28	9.59	11.73	0.695	0.70
					OCS-Ne				
10	88.6	292.2	0.20	317	0.67	1.72	2.14	6.16	14.50
11	111.0	294.2	0.16	247(248)	0.54	1.35	1.66	6.39	17.59
12	135.9	293.8	0.14	197	0.43	1.04	1.30	8.17	20.75
13	177.9	293.9	0.10	145	0.21	0.87	1.09	9.99	26.07
14	260.7	291.5	0.07	97	0.22	0.49	0.62	13.39	35.31
15	2242.0	293.0	0.009	11	0.02	0.08	0.01	52.01	129.61
16	280.0	293.1	0.07	91(92)	0.20	0.53	0.66	19.44	43.99
17	41.7	293.2	0.41	836	1.63	4.00	4.94	3.39	7.18

The initial temperature was 293 K in all runs;
The estimated errors were maximal : $\pm 2K$ for T, $\pm 1\%$ for U_p, $\pm 5\%$ for P, $\pm 3\%$ for D;

Table 2
Site-site (12-6) L-J parameters for Kr, Ne and OCS.

Parameter	Kr-Kr	Ne-Ne	O-O	C-C	S-S
ε [K]	164.4	33.7	78.0	29.0	178.0
σ [Å]	3.685	2.756	3.02	2.84	3.60

A difficulty often encountered in simulations of binary mixtures is that of an accurate description of the potential corresponding to the mixed interactions. Therefore, before leaving this section, attention will be paid to the potential model describing the interactions OCS-Kr and OCS-Ne.

It should, however, be borne in mind that, we do not aim to construct the real pair potential functions between the species in the mixtures. We are interested in effective pair potentials fitted to equilibrium properties at different thermodynamic conditions. In fact, the reliability of these models may be verified by testing them on the dynamical properties obtained from spectroscopic studies.

This procedure has been applied in our previous study on the OCS-Ar mixture. We found that our proposed potential, based upon the idea of the site-site interactions, predicts the structural and dynamical properties of the system in quite satisfactory accordance with experiment [1, 2].

Table 3
Structural parameters of the dimer structure of Kr-OCS and Ne-OCS.

Parameter	experimental [8]	Potential model of this work
R_{OCS-Kr} [Å]	3.806	3.782
$O-\widehat{c.m.}-Kr$ [^{o}]	74.1	78.08
Well depth [cm^{-1}]	-	-244.47
R_{OCS-Ne} [Å]	3.534	3.230
$O-\widehat{c.m.}-Ne$ [^{o}]	70.44	77.30
Well depth [cm^{-1}]	-	-111.12

In the present work, we chose this type of interaction model due to the existing similarities between the three mixtures. Thus, the 12-6 site-site Lennard-Jones potential parameters of OCS-Kr and OCS-Ne have been estimated on the basis of the well-known site-site potential model of pure OCS [10, 11] and of Kr and Ne [12–16] using the Lorentz-Berthelot combining rules. The obtained potential parameter values are presented in table 2. The structural parameters of the dimers OCS-Kr and OCS-Ne are summarized in table 3.

From the data in table 3 we conclude that the predictions obtained from the site-site L-J model are in close agreement with the experimental results. Moreover, additional calculation on the basis of the potential models A and B (see eq. 2 and 3 in I) and the predicted dimer structure of OCS-Kr and OCS-Ne, have shown that the obtained results are not satisfactory when compared with experiment and with those corresponding to the site-site model.

Finally, it is well known that another way of determining the interaction potential surface between two species is by *ab-initio* calculations. To the best of our knowledge, such calculation for OCS-Kr and OCS-Ne is not available in the literature. However, R. Bone [17] published a systematic *ab-initio* study on the potential energy surface of the Van der Waals dimer OCS-Ar. Although the results show a basis set dependence (see table 1 and 2 in ref [17]), the calculations which are based on a large basis set, find the minimum energy and the T-shaped structure in

close agreement with those observed experimentally [18] and those predicted using our site-site potential model [1].

These findings and the fact that the three mixtures are quite similar, led us in selecting the site-site potential model in order to describe the interactions between OCS-Kr and OCS-Ne in the MD simulation study of these diluted mixtures.

3. MOLECULAR DYNAMICS RESULTS

In the evaluation of the system properties, we used the equilibrium phase space production resulting from the MD runs. We first studied the density dependence of the equilibrium macroscopic properties of the mixtures. Subsequently our attention was focused on the dynamics of the linear solute molecules perturbed by the monoatomic solvents.

3.1. EQUILIBRIUM PROPERTIES

The calculated properties of interest for both systems are summarized in table 1 together with some experimental values. We compared these properties with the corresponding experimental data [20–23] and we found quite good agreement between them.

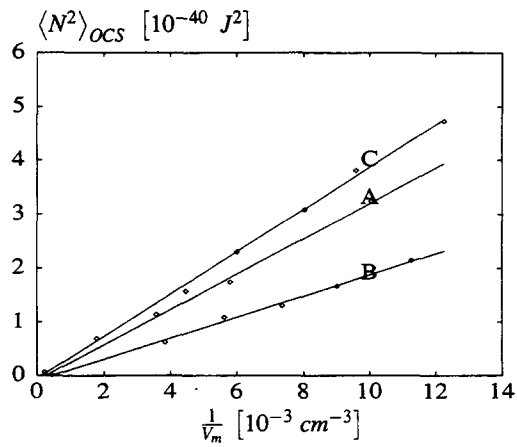

Figure 1. Mean squared torque of OCS as a function of reciprocal molar volume for its mixtures in Argon (A) [1], Neon (B) and Krypton (C).

Fig. 1 shows the behavior of the mean squared torque $\langle N^2 \rangle$ of the OCS molecule as a function of the reciprocal molar volume corresponding to the studied density range. A linear density dependence of this quantity is obtained. This behavior is also found experimentally from analyzing the ν_1 and ν_3 vibrations in the infrared spectra [4]. Moreover, as it is expected, we observe that for each mixture the corresponding straight line approaches zero at infinite densities. On the other side, from the above results it is obvious that the perturber strength increases in the following order : $Ne < Ar < Kr$, as expected.

3.2. INTERMOLECULAR STRUCTURE

The structure of the simulated mixtures is presented in terms of all static pair correlation functions (PCFs) $g_{\alpha\beta}(r)$. Due to the dilution of OCS molecule in both mixtures, the PCFs of interest are the following : (i) the center of mass (COM) functions, namely $g_{OCS-Kr}(r)$, $g_{OCS-Ne}(r)$, $g_{Kr-Kr}(r)$, $g_{Ne-Ne}(r)$ and (ii) the three site-site PCFs for each mixture $g_{S-X}(r)$, $g_{C-X}(r)$, $g_{O-X}(r)$, where X denotes the Kr or Ne atoms.

All these functions have been calculated for each simulated thermodynamic point. The characteristic extrema of these functions are summarized in table 4. Some of these PCFs are presented in figure 2 whereas the average number of neighbors in the first shell around each OCS molecule are also listed in table 4.

Table 4
Peak positions and amplitudes of the first maximum in the calculated PCFs together with the calculated coordination numbers of the first coordination shell of the OCS-R.g. and R.g.-R.g. PCFs.

OCS-Kr							
Run	$g_{Kr-Kr}(r)$	$g_{OCS-Kr}(r)$	$g_{S-Kr}(r)$	$g_{C-Kr}(r)$	$g_{O-Kr}(r)$	n_{Kr-Kr}	n_{OCS-Kr}
1	4.14:1.74	4.75:1.49	4.07:1.73	4.51:1.42	3.70:1.53	7.93	9.53
2	4.13:1.73	4.35:1.50	4.08:1.65	4.39:1.41	3.71:1.48	6.23	7.83
3	4.07:1.73	4.69:1.58	4.16:1.69	4.65:1.42	3.72:1.48	5.70	7.02
4	4.13:1.74	4.56:1.64	4.08:1.75	4.54:1.51	3.72:1.50	4.30	5.49
5	4.18:1.73	4.66:1.63	4.11:1.81	4.57:1.51	3.76:1.56	1.78	2.00
6	4.26:1.69	4.91:1.78	4.13:1.72	4.58:1.49	3.81:1.51	0.30	0.19
OCS-Ne							
Run	$g_{Ne-Ne}(r)$	$g_{OCS-Ne}(r)$	$g_{S-Ne}(r)$	$g_{C-Ne}(r)$	$g_{O-Ne}(r)$	n_{Ne-Ne}	n_{OCS-Ne}
10	3.07:1.19	4.19:1.26	3.70:1.25	4.33:1.16	3.21:1.13	3.34	5.68
11	3.12:1.18	4.33:1.23	3.66:1.25	4.54:1.18	3.25:1.12	2.68	4.62
12	3.04:1.15	4.35:1.27	3.69:1.23	4.42:1.18	3.33:1.09	2.22	3.84
13	3.10:1.54	4.37:1.22	3.10:1.19	4.58:1.13	3.38:1.06	1.64	3.01

We can use these results to obtain some conclusions. In both mixtures, the calculated coordination numbers show a strong density dependence. At high densities the first shell surrounding an OCS molecule in the mixture OCS-Kr contains 9.5 Kr atoms (Run 1) and in the mixture OCS-Ne contains 5.7 (Run 10) Ne atoms. These numbers are reduced to about 1 - 2 atoms at lower densities (Table 4). By inspecting the COM OCS-Kr and OCS-Ne PCFs we observe that these functions indicate some local structure at short distances. These characteristic features which broaden the first peak of these functions have been found at all thermodynamic states studied here. In fact, at each OCS-Kr and OCS-Ne PCFs we observe a small shoulder located at the left side of the first broad peak. The amplitude of the first peak shows a very small density dependence while its shape changes only somewhat at lower densities. Moreover, the coordination number calculated by integration of the COM PCFs up to the shoulder, is about 1-3 atoms at low and high densities. These numbers indicate the building of a T-shaped local structure

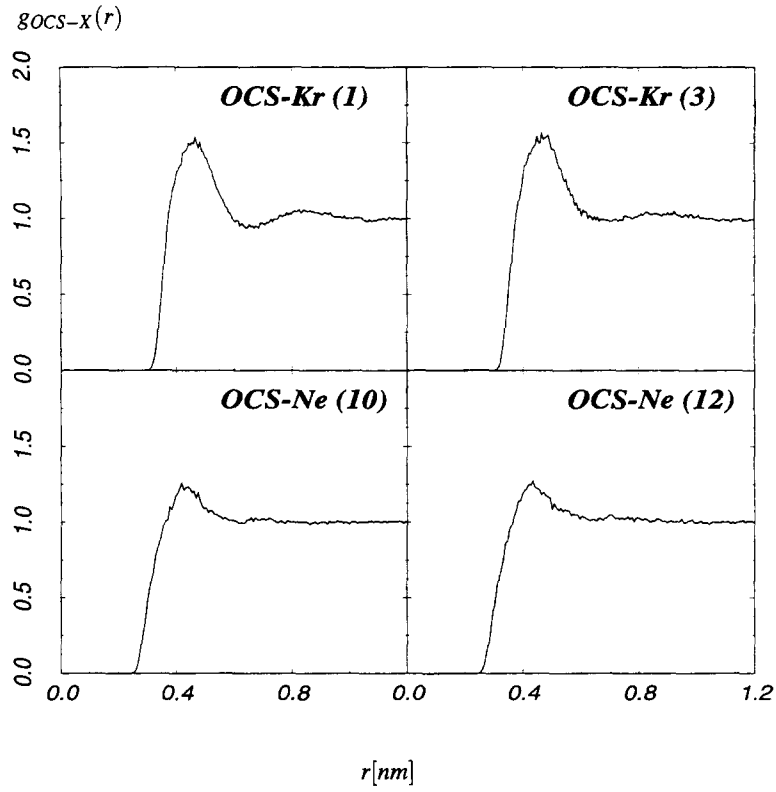

Figure 2. The simulated pair distribution functions $g_{OCS-X}(r)$, X=Kr, Ne for runs 1, 3, 10 and 12.

between an OCS molecule and the most nearly placed atoms. On the other hand, in order to describe the local structure in more detail, it is necessary to analyze the predicted atom-atom PCFs of the mixtures. This has been done by applying standard methodology as in the case of the mixture OCS-Ar [1]. These results are summarized in table 5. By inspecting the results from table 5 (see column two and three of each section) we conclude that for the mixture OCS-Kr and at short distances the Kr atoms attach to each OCS molecule close to the center of mass, building a T-shaped structure. Likewise, for the mixture OCS-Ne we found a similar structure except that the Ne atoms are closer to the C atoms.

The average duration of this structure was analyzed by calculating the time which the nearest solvent atoms spend in the inner subshell as in paper I. We found that for both mixtures the average duration is almost independent of the density. These results are summarized also in table 5.

Table 5
The average short distance structure and the average duration for the mixtures OCS-Kr and OCS-Ne. $O-\widehat{c.m.}-X$ denotes the angle between the axis of OCS and the unit vector along the intermolecular distance R_{OCS-X}, X= Ne, Kr.

Run	R_{OCS-Kr} [Å]	$O-\widehat{c.m.}-Kr$ [deg]	τ [ps]	Run	R_{OCS-Ne} [Å]	$O-\widehat{c.m.}-Ne$ [deg]	τ [ps]
	OCS-Kr				OCS-Ne		
1	3.636	86.7	0.407	10	3.17	87.8	0.315
2	3.646	87.0	0.401	11	3.18	87.9	0.315
3	3.641	86.7	0.418	12	3.18	88.2	0.319
4	3.653	87.0	0.405	13	3.19	88.1	0.338
5	3.657	86.8	0.432	14	3.19	88.0	0.321
6	3.670	87.6	0.460	15	3.21	89.6	0.338
7	3.644	87.0	0.401				

3.3. TRANSLATIONAL DIFFUSION

For the study of the single particle translational motion the relevant time correlation function is the center of mass linear velocity ACF

$$C_v(t) = \frac{\langle \mathbf{v}_i(0) \cdot \mathbf{v}_i(t) \rangle}{\langle \mathbf{v}_i^2(0) \rangle} \quad . \tag{1}$$

These functions have been calculated at each thermodynamic state of interest and the results are shown in Fig. 3. From the plots it is easy to see that the velocity ACFs decay faster as the density in both mixtures increases and that in the density range under study they do not exhibit a negative part. We have also studied the time evolution of these functions and we found that the translational dynamics may be successfully described in terms of a trial function consisting of two exponential terms with slowly decaying tails. This function has been proposed also in our previous treatment of OCS-Ar mixtures [2]

$$C_v(t) = (1-c)\left(1+\frac{t}{\tau_1}\right)e^{-\frac{t}{\tau_1}} + c\left(1+\frac{t}{\tau_2}\right)e^{-\frac{t}{\tau_2}} \quad . \tag{2}$$

The values of the parameters c, τ_1 and τ_2 which were obtained are listed in table 6 together with the overall correlation time τ_n. This time has been obtained in terms of the fit parameters by analytical integration of eq. 2

$$\tau_n = \int_0^\infty C_v(t)dt = 2\left(c(\tau_2-\tau_1)+\tau_1\right) \quad . \tag{3}$$

The remainder of this section will be devoted to the presentation and discussion of the calculated translational self-diffusion coefficient of the particles in the mixtures. The self-diffusion coefficient of OCS and Ar in this diluted mixture has also been included in the discussion for comparison. All calculations were based on the well-known equation :

$$D_s^x = \frac{1}{3}\int_0^\infty C_v^x(t)dt = \frac{2}{3}\left[c(\tau_2-\tau_1)+\tau_1\right]C_v^x(0) \tag{4}$$

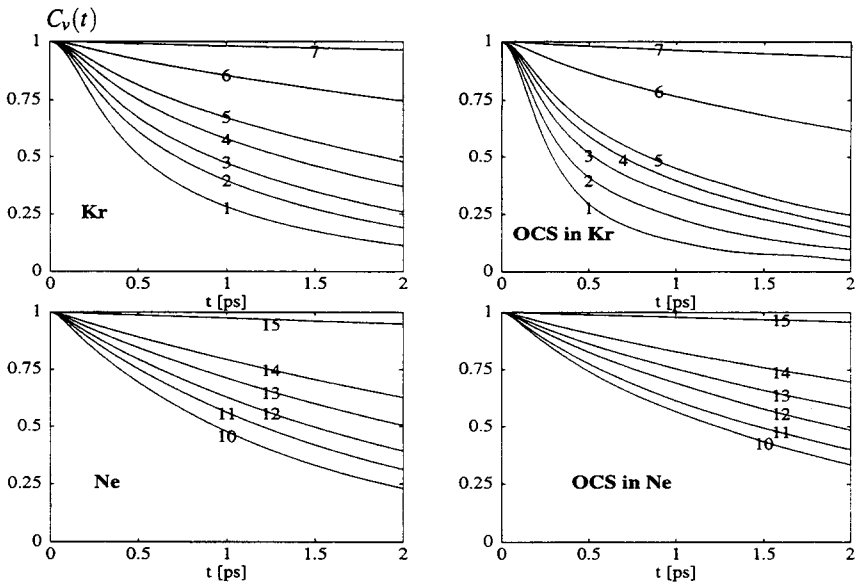

Figure 3. The center of mass linear velocity ACFs $C_v(t)$.

where $C_v^x(t)$ is the un-normalized COM linear velocity ACF of the mixture component x (x=OCS, Ne, Ar, Kr). This relation shows clearly the importance of the proposed trial function given by eq. 2 for the velocity ACFs to the problem of an accurate estimation of the diffusion coefficient. The obtained values for the mixtures are given in table 1 and they are also plotted vs. the reciprocal molar volume in figure 4. The results show the following qualitative behavior :

i the diffusivities decrease with increasing density. This feature reflects clearly the increase of the molecular caging in the mixtures at higher densities. Moreover, a non-linear density dependence of this quantity is obtained;

ii the mobility of the solvent atoms decreases more rapidly with density than that of the OCS molecules in the three mixtures;

iii by comparing the OCS diffusion coefficients D_s^{OCS} in the three mixtures in fig. 4d, we observe that over the whole density range, the D_S^{OCS} increases with the following order : $D_s^{OCS}(Ne) > D_s^{OCS}(Ar) > D_s^{OCS}(Kr)$;
and finally,

iv another feature of great interest here is that the mobility of these solvents is greater than that of the OCS molecules. Of course, this is not surprising in the case of the OCS-Ne and OCS-Ar mixtures due to the fact that the molar masses of Ne and Ar are smaller compared with the molecular mass of OCS. However, an unexpected result appears in the

Table 6
The fit parameters of the trial function (Eq. (2) to the simulated linear velocity ACFs for both mixtures. The second line for each Run corresponds to the parameters of the linear velocity of the solvent atoms.

Run	c	τ_1 [ps]	τ_2 [ps]	τ_n [ps]	Run	c	τ_1 [ps]	τ_2 [ps]	τ_n [ps]
		OCS-Kr					OCS-Ne		
1	0.301	0.127	0.526	0.494	10	0.298	0.915	0.134	1.521
	0.252	0.478	0.479	0.956		0.194	0.709	0.117	1.118
2	0.425	0.131	0.664	0.714	11	0.165	0.988	0.128	1.693
	0.413	0.821	0.183	1.104		0.163	0.843	0.123	1.452
3	0.545	0.135	0.729	0.918	12	0.134	1.192	0.139	2.103
	0.347	0.932	0.188	1.348		0.139	0.976	0.128	1.717
4	0.635	0.138	0.759	1.065	13	0.108	1.418	0.141	2.560
	0.259	1.107	0.191	1.739		0.109	1.199	0.134	2.166
5	0.684	0.146	0.817	1.209	14	0.069	1.757	0.141	3.290
	0.192	1.322	0.193	2.210		0.079	1.524	0.140	2.930
6	0.880	0.159	1.576	2.813	15	0.009	6.065	0.160	12.026
	0.083	2.302	0.202	4.255		0.011	5.434	0.161	10.755
7	0.983	0.160	4.637	9.126					
	0.011	7.394	0.210	14.630					

case of OCS-Kr mixture, where the D_s^{OCS} in Kr appear to lie always (in the density range under study) bellow the D_s^{Kr} though the molar mass of OCS is smaller than that of Kr.

The last observation, however, can not be tested against experiment since experimental self diffusion coefficients of OCS-Kr mixture are not available at present.

Further interpretation of these results is complicated by the fact that a number of molecular parameters characterizing the system can affect the diffusivity of a solute molecule. First of all, in a highly dilute solution the primary solvation shell of a solute molecule is constructed only from the solvent molecules. Thus, the most important interactions which affect the solute molecule are those between solute and solvent. Other factors of particular interest concerning this problem are, for example, the different size and geometrical shape of the solute and solvent molecules as well as their mass ratio. An investigation of all these parameters seems to be unattainable. At this stage one has the possibility to choose only one or two parameters and by systematic variation of them, keeping the rest constant, to estimate their influence on the diffusion process.

The above procedure has been applied successfully in previous computer simulation studies of transport properties of model fluids. However, in the case of binary mixtures these attempts were limited to mass and size ratio of hard spheres and LJ monoatomic components except the MD treatment of $C_6H_6 - SF_6$ [24]. In this study the molecular shape of both components has been explicitly taken into account and also site-site interactions have been applied.

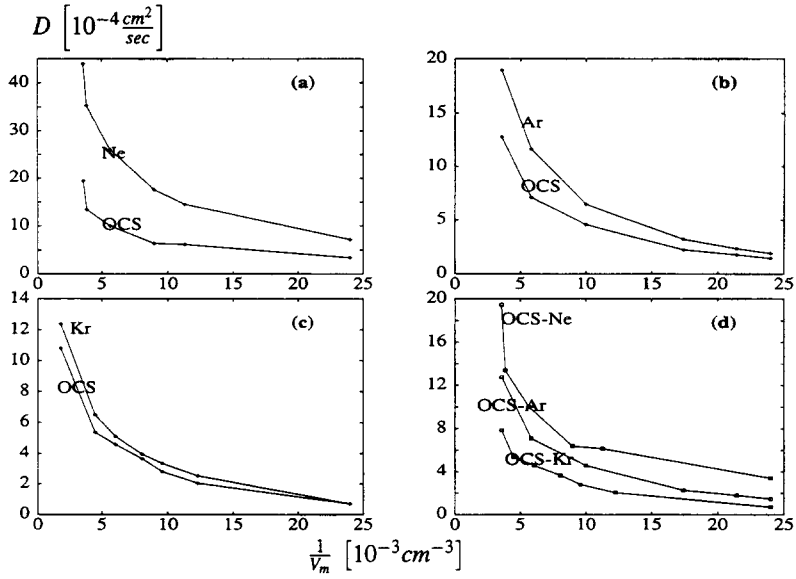

Figure 4. The calculated diffusion coefficient of solvents and OCS together with the diffusion coefficient of OCS in all the solvents.

Before proceeding further, we would like to pay attention to some remarkable experimental results for other molecular mixtures which were published a few years ago. In a systematic experimental work Schneider and co-workers [25] measured, by using super-critical fluid chromatography (SFC) technique, the diffusion coefficients of various organic substances highly diluted in dense chlorotrifluoromethane ($CClF_3$) as well as in sulfurhexafluoride (SF_6). The measurements were carried out at temperatures from 283 to 338 K and at densities from 0.4 to 1.0 gr/cm^3 for $CClF_3$ and from 0.3 to 1.4 gr/cm^3 for SF_6. The most noticeable result in this study was that of the self-diffusion coefficient of SF_6 $D_s^{SF_6}$ [26] comparing to the coefficient of the highly diluted solutes benzene, methylbenzene, 1,4 dimethylbenzene and 1,3,5 trimethylbenzene. In all these highly diluted solutions which correspond practically to the pure liquid as well as supercritical SF_6, the $D_s^{SF_6}$ *"lie well above"* the measured coefficient of the solute molecules though the molar mass of SF_6 is greater than those of the solutes.

This experimental result exhibits similar behavior with our MD prediction upon the OCS molecules dissolved in Kr under pressure. It may be mentioned that there is no appropriate formalism which could be applied in order to study theoretically this diffusion behavior of the solutes in these highly diluted solutions. At this stage the authors in [25] did not attempt to analyze these results in terms of any theoretical framework. However, they tried to explain the above effect by taking into account the more compact SF_6 molecular shape compared to those of the organic solutes. In that sense, they assumed that the "more compact shape of SF_6 compensates for its large mass resulting in an overall higher mobility". In a subsequent

MD treatment of the dilute solution $C_6H_6 - SF_6$ [24] C. Hoheisel investigated the self-diffusion coefficient of both components at thermodynamic states such as in the real experiment. The most interesting result obtained in this treatment is that the density dependence of the calculated diffusivities shows the behavior of experimental results. Moreover, the effect of the molecular shape on the diffusion in this fluid has been also partially investigated.

In what follows we shall try to explain the diffusion behavior of the components in OCS-Kr solution. In particular, we focus on the effect of the solute shape on this transport property. As a first step in investigating this problem we have extended our calculations on the OCS-Kr system by carrying out additional MD runs where both bond lengths of OCS molecule have been reduced (model b) or extended (model c) to about 30% while all other system parameters being kept fixed. Each artificial model solution was simulated at two thermodynamic states corresponding to the molar volumes of 41.7 and 280 cm^3/mol and temperature of 293 K. The diffusion coefficients D_s^{OCS} and D_s^{Kr} of the mixture components were calculated following the above described procedure. We can now make some comments based on the diffusion values in connection with the diffusion coefficients from the pure model solutions. As it is expected, by comparing the diffusion coefficients of Kr from the three model solutions to each other and at the same thermodynamic state, we find their values in quite good accordance. It is of course due to the fact that the potential model describing the Kr-Kr solvent interactions has been not changed for the pure model solutions.

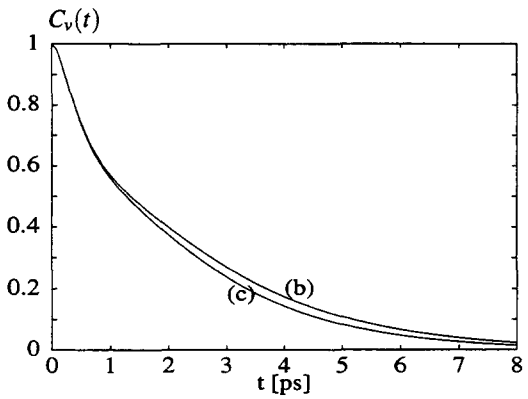

Figure 5. The calculated linear velocity ACFs of OCS $C_v^{OCS}(t)$ for artificial models (b) and (c) at $V_m = 280\frac{cm^3}{mol}$ and 293 K.

At relatively high density ($V_m = 41.7\frac{cm^3}{mol}$) we find that the diffusion coefficient of OCS is practically equal for pure model (a) and model (b) while it is slightly smaller for model (c). At lower density ($V_m = 280\frac{cm^3}{mol}$) the calculated diffusion coefficient is smaller for the model (c) while it is larger for model (b) compared with the pure model (a). From the above results we see clearly that the mobility of OCS in model solution (b) is larger, while in model (c) is smaller

with respect to its mobility in pure model (a). In other words, we may conclude that the mobility of OCS molecule in a thermal bath of monoatomic solvents under pressure will be affected by its linear shape more negatively than that of another, of equal mass but less anisotropic solute. This MD finding confirms the theoretical prediction on the self-diffusion in molecular liquids published a few years ago by D. Chandler [27]. This theory is based on a rough hard sphere model and takes into account the coupling between translational and rotational motion of the molecules. This mechanism affects the relaxation behavior of the linear velocity ACF of the anisotropic molecules and consequently their diffusivity. It has been shown that this coupling has an effect of reducing generally the translational diffusion coefficients. Figure 5 illustrates the calculated linear velocity ACFs of OCS in Kr for the artificial models (b) and (c) at 293 K and $V_m = 280\frac{cm^3}{mol}$. The purpose of the comparison in this figure is to bring forth the difference between these two normalized ACFs. Thus, the curve corresponding to the more anisotropic OCS model (c) decays faster than the curve of the model (b). Of course, this difference is more evident at longer times, while both curves initially and approximately up to the time of 1 ps show a similar decay.

4. CONCLUDING REMARKS

In this work we have presented MD simulation results for diluted mixtures of OCS with monoatomic solvents at room temperature and at a rather wide density range. The results obtained were based on the site-site (12-6) L-J potential models. The thermodynamic results for the mixtures are in quite good agreement with experiment.

The results of this work can be summarized as follow :

i The site-site LJ potential models proposed in these MD studies between an OCS molecule and the monoatomic solvents Ne, Ar, Kr describe successfully the experimental thermodynamic properties of the mixtures.

ii The local intermolecular structure of the OCS solute with the solvent atoms has been studied by analyzing the calculated COM and the site-site PCFs. These functions show clearly a characteristic density dependence. In all cases we found that the most probable configuration between an OCS molecule and the nearest solvent atoms is a nearly T-shaped structure. At low densities this structure is 1:1. At relative higher densities the structure is extended to 2 or 3 solvent atoms. The most stable structure is that of the mixture OCS-Kr.

iii The calculated mean-squared torque on OCS from the solvents show a linear dependence on the density. This behavior has also been obtained from IR spectroscopy.

iv The translational diffusion coefficients of both components in the three mixtures have been obtained and discussed. They decrease with increasing the density. A non-linear density dependence of these data is obtained. The mobility of the solvents decreases more rapidly than that of the solutes in the three mixtures. The D_s^{OCS} in the mixtures increases with the following order : $D_s^{OCS}(Ne) > D_s^{OCS}(Ar) > D_s^{OCS}(Kr)$. Finally, the most interesting result here is that the mobility of Kr is greater than that of OCS, though the molar mass of the solute is smaller than that of Kr. This result has been explained in terms of microscopic dynamics of the molecules.

Acknowledgements

This work was carried out within the project No. 91 $E\Delta$ 111. The financial support of the Greek Ministry of Energy and Technology is gratefully acknowledged. The CPU time allocation on CONVEX C3820 of the Computer Center of the University of Athens and on CONVEX C3820 of the Supercomputing Center NCSR DEMOKRITOS Athens, Greece is also gratefully acknowledged.

REFERENCES

1 J. Samios, D. Dellis, H. Stassen, Chem. Phys. **178** (1993) 83
2 D. Dellis and J. Samios, Chem. Phys. **192** (1995) 281
3 C. Dreyfus, E. Dayan, J. Vincent-Geisse, Mol. Phys. **30** (1975) 1453
4 C. Dreyfus, L. Berreby, E. Dayan and J. Vincent-Geisse, J. Chem. Phys. **68** (1978) 2630
5 D. Clermontel, H. Vu, B. Vodar, J. Quant. Spectrosc. Radiat. Transfer, **16** (1976) 695
6 C. Dreyfus, L. Berreby, T. Nguyen-Tan., J. Chem. Phys. **76** (1982) 755
7 T. J. Balle, W. H. Flygare, Rev. Sci. Instr. **52** (1981) 33
8 F. J. Lovas, R. D. Suenram, J. Chem. Phys. **87** (1987) 2010
9 G. D. Hayman, J. Hodge, B. J. Howard, J. S. Muenter, T.R. Dyke, Chem. Phys. Lett. **118** (1985) 12
10 J. Samios, H. Stassen, Th. Dorfmüller, Chem. Phys. **160** (1992) 33
11 H. Stassen, Th. Dorfmüller, J. Samios, Mol. Phys. **77** (1992) 339
12 J. V. Hirschfelder, C. F. Curtiss, R. B. Bird, *Molecular Theory of Gases and Liquids*, W. Inter. (1967)
13 C. Hoheisel, U. Deiters, Mol. Phys. **37** (1979) 953
14 C. Hoheisel, Phys. Chem. Liq. **9** (1980) 245
15 G. G. Gray, K. E. Gubbins, *The theory of molecular liquids*, Academic Press, Oxford (1984)
16 M. Rigby, E. B. Smith, W. A. Wakeman, G. C. Maitland, *The forces between Molecules*, Clanderon Press, Oxford (1986)
17 R. G. A. Bone, Chem. Phys. **178** (1994) 255
18 S. J. Harris, K. C. Janda, S. E. Novick, W. Klemperer, J. Chem. Phys. **63** (1975) 881
19 A. Michels, T. Wassenaar, P. Louwerse, Physica, **XXIV** (1958) 769
20 A. Michels, T. Wassenaar, P. Louwerse, Physica **26** (1960) 539
21 A. Michels, T. Wassenaar, G. J. Wolkers, Physica **31** (1965) 237
22 J. A. Beattie, J. S. Brierley, R. J. Barriault, J. Chem. Phys. **20** (1952) 1613
23 J. A. Beattie, J. S. Brierley, R. J. Barriault, J. Chem. Phys. **20** (1952) 1615
24 C. Hoheisel, J. Chem. Phys. **89** (1988) 7457
25 A. Kopner, A. Hamm, J. Ellert, R. Feist, G. M. Schneider, Chem. Eng. Sci. **42** (1987) 2213
26 P. G. Zykov, P. I. Bogdanov, A. S. Rasponin, Z. h. Tekh. Fiz. (Soviet Phys. Tech. Phys.) **25** (1980) 362
27 D. Chandler, J. Chem. Phys. **62**, (1975) 1358